Snow dunes and glazed surfaces in Antarctica: new field and remote-sensing data

MASSIMO FREZZOTTI,[1] STEFANO GANDOLFI,[2] FLORIANA LA MARCA,[3] STEFANO URBINI[4]

[1]*ENEA, Centro Ricerche Casaccia, P.O. Box 2400, I-00100 Rome, Italy*
[2]*DISTART, Università di Bologna, Viale Risorgimento 2, I-40136 Bologna, Italy*
[3]*Dipartimento di ICMMPM, Università di Roma "La Sapienza", Via Eudossiana 18, I-00184 Rome, Italy*
[4]*Istituto Nazionale di Geofisica e Vulcanologia, DIPTERIS, Università di Genova, Viale Benedetto XV 5, I-16134 Genoa, Italy*

ABSTRACT. As part of the International Trans-Antarctic Scientific Expedition project, the Italian Antarctic Programme undertook two traverses from the Terra Nova station to Talos Dome and to Dome C. Along the traverses, the party carried out several tasks (drilling, glaciological and geophysical exploration). The difference in spectral response between glazed surfaces and snow makes it simple to identify these areas on visible/near-infrared satellite images. Integration of field observation and remotely sensed data allows the description of different mega-morphologic features: wide glazed surfaces, sastrugi glazed surface fields, transverse dunes and megadunes. Topography global positioning system, ground penetrating radar and detailed snow-surface surveys have been carried out, providing new information about the formation and evolution of mega-morphologic features. The extensive presence, (up to 30%) of glazed surface caused by a long hiatus in accumulation, with an accumulation rate of nil or slightly negative, has a significant impact on the surface mass balance of a wide area of the interior part of East Antarctica. The aeolian processes creating these features have important implications for the selection of optimum sites for ice coring, because orographic variations of even a few metres per kilometre have a significant impact on the snow-accumulation process. Remote-sensing surveys of aeolian macro-morphology provide a proven, high-quality method for detailed mapping of the interior of the ice sheet's prevalent wind direction and could provide a relative indication of wind intensity.

INTRODUCTION

The snow deposition process is very complicated on the Antarctic Plateau, because blowing snow is intense, accumulation is low, and snow remains in the form of aeolian particles on the surface. Snowdrift transport changes the topography, and the topography alters the wind field again in a feedback system between the cryosphere and atmosphere. Many types of surface features, such as sastrugi, snow dunes, pitted patterns and glazed surfaces, are distributed on the surface of the Antarctic ice sheet in varying degrees of scale and frequency as a result of interaction between the atmosphere and the ice-sheet surface. Recently, extensive snow megadunes have been described. These features occupy $> 500\,000\,km^2$ and are oriented perpendicular to the regional katabatic wind direction (Fahnestock and others, 2000b; Frezzotti and others, in press).

As part of the International Trans-Antarctic Scientific Expedition (ITASE) project, the Italian Antarctic Programme undertook two traverses from the Terra Nova Bay station (TNB; 74°41′S; 164°06′E) to Talos Dome (TD; 72°48′S; 159°06′E; 2316 m) and to Dome C (DC; 75°06′S; 123°23′E; 3232 m). The scientific objectives of the traverse programme were to develop a high-resolution interpretation and three-dimensional map documenting the last 200–1000 years of climate, atmospheric and surface conditions over the eastern DC drainage area.

The traverse to TD was performed from 3 to 30 November 1996, and the distance covered was about 600 km (Frezzotti and others, 1998). The traverse to DC started from GPS1 on 19 November 1998 and reached DC on 5 January 1999 after 1300 km (Fig. 1). The first 400 km of the traverse followed the same route (up to 31Dpt) as the 1996 traverse (Frezzotti and others, 1998). Along the traverse, the party carried out several tasks (drilling, glaciological and geophysical exploration,
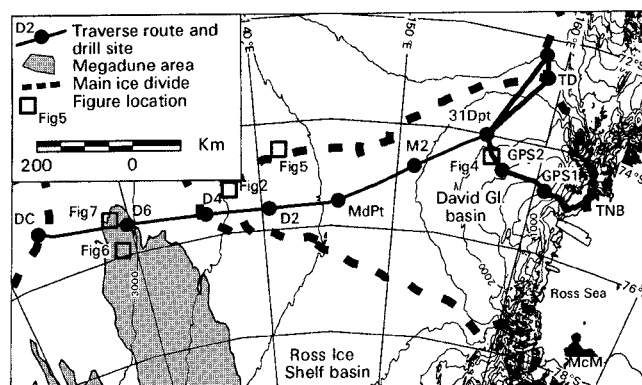
Fig. 1. Schematic map of the PNRA–ITASE traverse route, including firn-core location (drill sites), megadune area, main ice divide and figure locations. 31Dpt, 31 Deposit; DC, Dome C; McM, McMurdo; MdPt, Midpoint; TNB, Terra Nova Bay station; TD, Talos Dome.

etc.). The route was identified and surveyed in Italy from georeferenced satellite image analysis (Landsat Thematic Mapper (TM), European Remote-sensing Satellite-1 (ERS-1) synthetic aperture radar (SAR) and Advanced Very High Resolution Radiometer (AVHRR)) and using a digital elevation model (DEM) derived from an ERS-1 radar altimeter (Rémy and others, 1999).

In most of the East Antarctic plateau there are no meteorological records, and it is only at particular times of year that effective ground-based research can be carried out, due to the harsh climate and the lack of daylight. Remote-sensing analysis can provide information about the surface wind field through the survey of location, direction and areal extent of surface features formed by aeolian processes (Bromwich and others, 1990; Frezzotti, 1998). This paper combines field observations and remotely sensed data to describe surface morphology along the traverse, provides new information about processes of formation of aeolian features, and carries implications for snow accumulation, distribution and variability. On the local scale, there is continual interaction among processes such as wind, radiation balance and temperature variations of the snow surface; in particular, the surface energy balance and katabatic wind patterns are highly interrelated. Smooth and glazed surfaces should also be considered types of surface features, although they differ from other types which are generally distributed in a zonal form with a certain width and orientation. The morphology and formation of snow surface micro-relief in Antarctica has been well documented by numerous workers (e.g. Watanabe, 1978; Goodwin, 1990). In this paper we focus on the macro-morphology of the surface of the Antarctic ice sheet surveyed by satellite image analysis and recognized and studied in field surveys.

METHODOLOGY

Remote sensing

The location of macro-relief features (glazed surfaces, transverse dunes, megadunes, glazed-surface sastrugi fields) and their direction and extent were determined by remote-sensing analysis.

In this study we have integrated field surveys with satellite images of Landsat 4 and 5 TM (66/113, 20 February 1992; 72/113, 13 January 1992; 78/113, 15 January 1992; 81/113, 20 January 1992; 84/113, 17 January 1992), Landsat 7 Enhanced Thematic Mapper Plus (ETM+) (81/114 and 81/115, 2 January 2000) and U.S. National Oceanic and Atmospheric Administration (NOAA) 12–14 AVHRR (November 1994– November 1999). The Landsat TM and ETM+ have a pixel resolution of 30 m and seven spectral bands: three in the visible wavelength region (bands 1–3), three in the near-infrared wavelength region (bands 4, 5 and 7) and one region of thermal infrared wavelength (band 6). The Landsat 7 ETM+ has panchromatic band with a higher pixel resolution of 15 m. Landsat images were georeferenced by means of geographical coordinates derived from the satellite ephemeris; the geolocation of ETM+ has a 1σ error of 50 m (personal communication from R. Bindschadler, 2000). The AVHRR images were collected by the high-resolution picture transmission (HRPT) receiving station installed at TNB. AVHRR sensors installed on NOAA's satellite have a pixel resolution of 1.1 km at nadir in five

spectral bands: visible red (band 1), near-infrared (band 2), middle infrared (band 3) and thermal infrared (bands 4 and 5). More than 200 AVHRR images from NOAA 12–14 meteorological satellites, with < 30% cloud cover over the plateau, were analyzed, having been selected from those acquired by the HRPT station from 1994 to 1999. In this study we used the images acquired by NOAA 14 on 16 November 1995 (0505 h GMT; solar azimuth 308°; solar elevation 30°). The ephemeris-based geolocation is accurate to only about ±3 km (Fahnestock and others, 2000a), so the re-projection was performed using the Antarctic Digital Data Base (BAS and others, 1993) and DEM provided from Rémy and others (1999). The projection used is polar stereographic from the World Geodetic System (WGS84) ellipsoid, with the plane of projection parallel to 71° S.

The satellite images were analyzed, compared and organized into a geographic information system (GIS) using ERDAS, TerraScan and ARCINFO software. Image processing included routine procedures such as radiometric corrections, noise and striping removal, and application of special linear stretches of individual bands after inspection of grey-value histograms to enhance surface features and characteristics.

Field survey

A spatial distribution survey of the micro-relief surface type, size and orientation was conducted along the route during the austral spring–summer (November–December). The spring season provided the best opportunity to investigate micro-relief development and distribution, because the observed micro-relief formed during winter, when most annual precipitation and the strongest katabatic surface winds occur (Goodwin, 1990). The roughness of the snow surface, as well as the orientation and size of the surface relief, was measured over 500 m × 500 m quadrates at intervals of 5 km along the traverse and continuously along some profiles in the megadune area. The micro-relief features observed were classified according to the system described by Fujiwara and Endo (1971) and applied to Japanese and Australian Antarctic Research Expedition (JARE and ANARE) traverses inland in the plateau region of Dronning Maud Land and Wilkes Land (Goodwin, 1990). The mean azimuths of the micro-relief were measured by magnetic compass and converted into true bearings by GPS, and the mean height of the micro-relief was recorded using a ruler. The surface micro-relief observed is divided into three types (Watanabe, 1978; Goodwin, 1990):

> depositional features formed from wind-transported friable snow (barchanoid, dune, etc.);
>
> redistribution features formed as a result of erosion of depositional features (sastrugi, pits, etc.);
>
> erosional features formed from the long-term exposure to katabatic winds (glazed surfaces).

In the first 400 km, the 1998/99 data show the same general orientation in sastrugi directions and types that were noted during the 1996 expedition.

Surface elevation profiles and local topography along the traverse TNB–DC was measured by global positioning system (GPS) (Urbini and other, 2001), whereas regional surface topography was analyzed using a DEM of Antarctica with digitized element resolution of 1 km, provided by Rémy

and others (1999). A 3 × 3 pixel window (pixel size: 1 × 1 km) was used to calculate the slope of each pixel using the DEM. A GPS survey was performed along the traverse using two master stations located at the beginning (TNB) and at the end of the traverse (DC). During the megadune survey a master station at D6 (site of field camp) was used. Data acquired from master stations were utilized in post-processing to obtain an accurate location of the entire track (Urbini and others, 2001). The mobile receivers, equipped with geodetic antennas, were installed on vehicles and were used for the kinematic surveys to perform altimetric profiles and to correct ground-penetrating radar (GPR) acquisition as a function of both ellipsoidal height and surface coordinates. The accuracy of the altimetric profile along the traverse is mainly due to the distance between the master and rover stations and varies between <1 m and 3 m at the farthest point. However, the accuracy of the altimetric profile performed at the megadune area, using the D6 master station, is up to 10 cm. Vehicle and thus GPS antenna speed oscillated from about 8 to 12 km h^{-1}. The sampling rate of the GPS receivers (master and rover) was fixed at 5 s; meaning about one coordinate every 10–15 m.

GPR along continuous profiles provides detailed information on spatial variability in snow accumulation (Richardson and others, 1997; Richardson and Holmlund, 1999; Urbini and others, 2001). Data acquisition was performed along the TNB–DC traverse with a GSSI SIR10B unit equipped with one monostatic antenna with a central frequency of 400 MHz. The mainframe unit was mounted inside the vehicle (Pisten Bully 330D) cabin together with a geodetic GPS instrument, while the antenna was pulled on a small wooden sledge. Principal acquisition parameters were 150 ns for the vertical investigation range and 1–5 scan s^{-1} for the acquisition rate (15–20 m). Vehicle and thus antenna speed oscillated from about 8 to 12 km h^{-1}, meaning about one scan every 2–3 m (with the acquisition rate at 1 scan s^{-1}) and 0.4 to 0.7 m (with the acquisition rate at 5 scan s^{-1}). For electromagnetic wave-speed calculations the depth–density relation for the snowpack was established using the density profile of 20 firn cores (12–52 m deep), retrieved with an electromechanical drilling system (diameter 100 mm). The integration of GPS and GPR provided the ellipsoidal height of both the topographical surface and firn stratigraphy. Urbini and others (2001) describe the GPR methods in detail. In line with Vaughan and others (1999), we assume that layers that produced a strong radar reflection are isochronous.

DISCUSSION

Aeolian distribution

Landsat TM image analysis showed a lower albedo or reflectivity of glazed surfaces compared with snow and blue ice (Fig. 2). Firn and ice albedos generally decrease passing from the visible to the near-infrared wavelengths (e.g. Warren, 1982), whereas glazed surfaces present spectra reflectance intermediate between snow and ice. The spectral difference between snow and glazed surfaces makes it simple to identify these areas on false-colour image composite TM images with bands 2–4 (Fig. 2). Orheim and Lucchitta (1987) pointed out that ratioing satellite bands is a useful technique for extracting information regarding surface properties because it accentuates the albedo signal by reducing the slope effects. An evaluation of NOAA
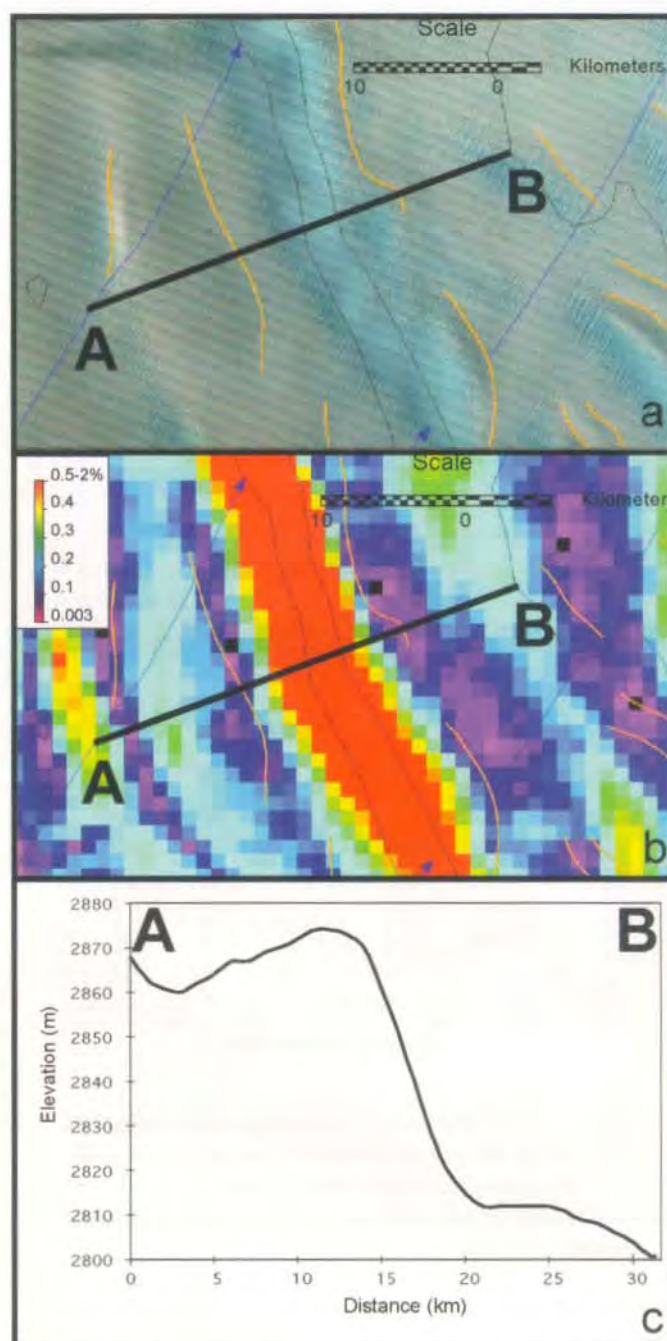

Fig. 2. (a) Subscene of Landsat TM image in false colour (RGB, 4, 3, 2) showing a wide glazed surface area of the plateau with glazed surfaces (blue in image) and snow (grey), transverse dunes (orange lines) and directions of wind inferred from satellite image (blue line). (b) Slope map of area in (a) produced from DEM. (c) Elevation along A–B profile produced from DEM.

AVHRR and Landsat TM images shows that the AVHRR band 2/1 ratio provides a good visual separation between glazed surfaces and snow. Figure 3 shows the satisfactory congruence between the spatial distribution along the traverse of erosional features (glazed surfaces) and the slope and the ratio of AVHRR band 2/1.

An important observation from the micro-relief survey is that whilst the redistribution and erosional features are spatially continuous up to 1000 km, depositional micro-reliefs only extensively occur close to the David Glacier ice divide at 810 km and in the last 200 km (Fig. 3). Between
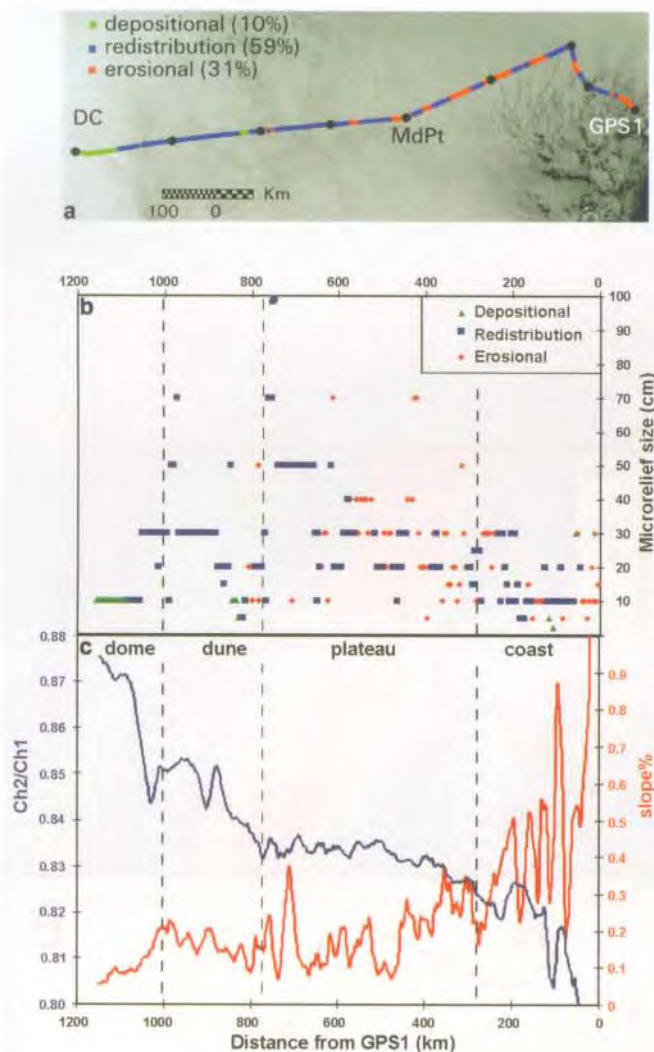
Fig. 3. (a) AVHRR band 2/1 ratio image of the traverse area from TNB to DC and micro-relief surveyed along the traverse. (b) Micro-relief size and distribution along the traverse. (c) Slope produced from DEM and the band 2/1 ratio along the traverse.

the valleys and on the leeward sides of nunataks (Frezzotti, 1998) in the mountainous area of TNB.

Remote-sensing and field data along the traverse TNB–DC indicate four sectors (Fig. 3):

the coastal area between GPS1 and about 220 km, characterized by a steep slope of up to 2.5%, by erosional and redistribution micro-reliefs and by a low value of AVHRR band 2/1 ratios;

the plateau area up to 780 km from GPS1, with a slope of up to 0.45%, characterized primarily by redistribution of micro-reliefs and secondarily by erosional features and an intermediate value of AVHRR band 2/1 ratios;

the megadune area between 780 and 1000 km, with a more homogeneous value in slope (0.2–0.1%) and in AVHRR band 2/1 ratios;

the dome area in the last 200 km, with a slope of <0.15%, characterized by depositional features.

Remote-sensing analysis of the plateau area integrated with field data allowed the survey of the following macro-morphology: drift plumes and snowdrifts, wide glazed surfaces, sastrugi glazed surface fields, transversal dunes, and megadunes.

Drift-plume, snowdrift and blue-ice areas have been surveyed in the mountain area up to 2200 m a.s.l.; these features have been extensively studied by Bromwich and others (1990) and Frezzotti (1998). In this paper we investigate the unexplored part of the plateau.

A wide glazed surface is an extensive area (several km²) where the surface is characterized by glazing (Fig. 2). A wide glazed surface presents cracks (up to 2 cm), with patterns in polygonal form, that could be correlated to a long-term hiatus in snow accumulation (Watanabe, 1978). Glazed surfaces were one of the common features observed along the traverse and consist of a single snow-grain thickness layer cemented by thin (0.1–2 mm) films of regelated ice. Trenches cut in mound slopes of wide glazed surface show the depth-hoar layer (up to 2 m) penetrated by iced crust with a very coarse snow grain-size (up to 2 mm). Under strongly developed glazed surfaces the depth-hoar layer clearly indicates prolonged sublimation due to a hiatus in accumulation and therefore a long, multi-annual, steep temperature-gradient metamorphism (Gow, 1965). Long-term hiatus forms do not allow the burial of snow layers by accumulation in subsequent years. The sublimation and upward transport of water vapour belonging to the subsurface snow layer causes the condensation of vapour (recrystallization) on the lower part of the ice crust (Fujii and Kusunoki, 1982). The glazed surface forms on the surface following the kinetic heating of saltant drift snow under constant katabatic wind flow (Goodwin, 1990) and the condensation–sublimation process on both sides of the crust (Fujii and Kusunoki, 1982). Fujii and Kusunoki (1982) determined a density value of 0.69 g cm⁻¹ from the glazed surface at Mizuho station. GPS and GPR profiles of a wide glazed surface, located on the traverse between GPS2 and 31Dpt (Fig. 1), show excellent resolution of sedimentary structures that could be correlated with long-term hiatus forms or with low or lack of accumulation processes (Fig. 4). The mass balance of this wide glazed surface is nil or slightly negative. Integration of satellite images with slope and field-survey data indicated that the glazed surfaces are present in a wide area of the plateau where the slope is higher than 0.25° (0.4% or 4 m km⁻¹). Figures 2 and 4 show slope and elevation profiles of

Midpoint (MdPt) and DC, the micro-reliefs are mostly of the redistribution and depositional type. The erosional features, between the David Glacier ice divide and DC, are present only on the leeward side of megadunes. The ice divide between David Glacier and the Ross Ice Shelf basins (Fig. 1), along the traverse, is a flat area (810 km from GPS1), and the difference in elevation between the two basins is <10 m, characterized by a low slope (<0.1%) similar to the DC area. Along the traverse TNB–DC, erosional features (glazed surfaces) constitute 31%, redistribution features (sastrugi) 59% and depositional features only 10% of micro-reliefs. The average height of micro-relief distribution shows very high variability, including an increase in height from 400 km to 1000 km from GPS1 (Fig. 3). Slope and AVHRR band 2/1 ratio profiles and micro-relief surveys show very high variability along the coastal and plateau areas, and homogeneous characteristics in the dome area. The lower value of AVHRR band 2/1 ratio is present in the first 300 km of traverse where the katabatic wind model of Bromwich and others (1990) shows speeds of 8–16 m s⁻¹. The intensity and persistence of predominantly wintertime katabatic winds has created an extensive blue-ice area along
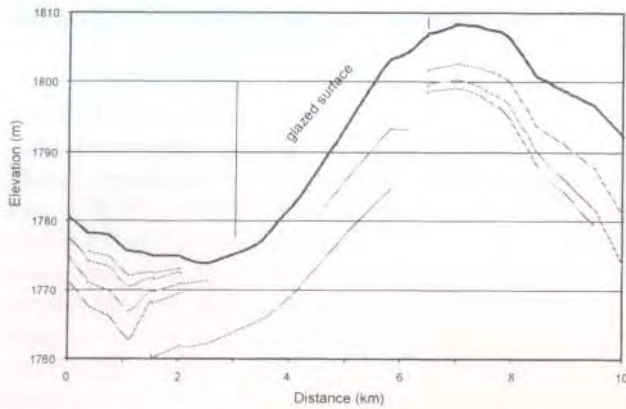
Fig. 4. GPS and GPR profiles of wide glazed surface show the reduction of thickness and disappearance of the snow layer in the wide glazed surface that could be correlated with long-term hiatus in accumulation.

Fig. 5. Subscene of Landsat TM image in false colour (RGB, 4, 3, 2) showing an area of plateau with a sastrugi glazed surface field; the arrow shows the prevailing wind direction.

the wide glazed surface, where the correlation between the presence of wide glazed surface and the increase of slope in the downwind part is obvious.

The drainage basin of the glaciers that drain into Terra Nova Bay is about 235 000 km^2 in area (Frezzotti and others, 2000), about 30% of which presents a slope of >0.4%. Stake measurements performed in the traverse from GPS1 to 31Dpt showed a large spatial variability, with ablation values up to 13 kg m^{-2} a^{-1} in the wide glazed surface area. Frezzotti and others (2000) pointed out that the ice discharge of glaciers draining into TNB is less than half that required for a zero net surface mass balance, according to the inputs given by the accumulation estimates widely adopted at present. The explanation for this large apparent imbalance is probably an overestimation of snow accumulation using historical data from snow-pit stratigraphy, as pointed out by Stenni and others (in press), and the extensive presence of wide glazed surface in the basin with nil or slightly negative snow accumulation.

Sastrugi glazed surface fields have the typical texture of a seasonal feature, with a relatively flat horizontal plane and a thin and soft glazed surface. Sastrugi glazed surface fields have been frequently surveyed along the traverse in the plateau part (300–900 km), and they are the most common macro-morphological structure observed along the traverse and surveyed from satellite images. The surface conditions are characterized by the alternating occurrence of wide, smooth surfaces (glazed surfaces) and wide, rough surfaces (sastrugi zones) with a distinct boundary (Fig. 5) and a nearly uniform width for considerable distances. Sastrugi glazed surface fields are characterized by the alternation of sastrugi fields with sporadic longitudinal dunes (10–20 m long and a few metres wide), measuring up to 1 m in height, and flat glazed surfaces with sporadic sastrugi. The field's boundaries are roughly linear, with the line of elongation parallel to sastrugi direction and therefore to the prevailing wind direction. Sastrugi glazed surface fields are typically several kilometres long and 100–200 m wide, cover several hundred km^2 and are similar to longitudinal sand dunes in satellite images (Fig. 5). The regional slope of a sastrugi glazed surface field area is generally <0.3%. One of the most important pieces of positive feedback is the smoothness and low albedo of the glazed surface compared to the roughness and albedo of the surrounding sastrugi field, causing the wind to be stronger over the glazed
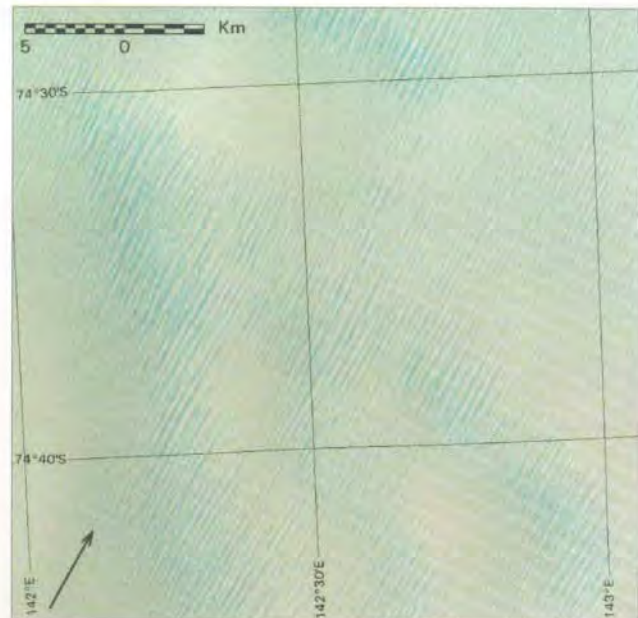
surface than over the sastrugi (Fujii and Kusunoki, 1982; Van den Broeke and Bintanja, 1995). As hypothesized for longitudinal sand dunes (Houbolt, 1968), pressure exists between the axes of the inter-dunes (glazed surfaces) and the crest of the dunes (sastrugi fields); these pressure gradients are caused by the sastrugi's resistance to the wind. This results in the formation of "long vortex airflows" in the glazed areas, which give the wind an overall spiral motion directed outward at ground level towards the sastrugi, with transportation of snow from the glazed surfaces to the sastrugi fields. Vortices may also control the migrations of sastrugi fields along the wind direction.
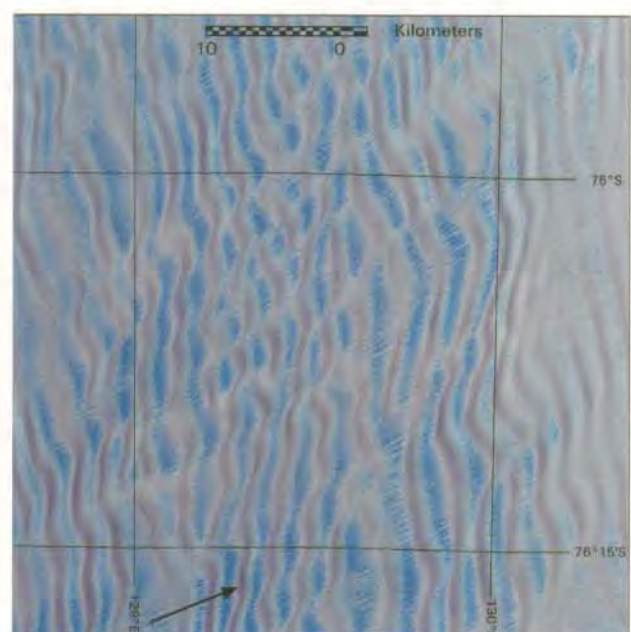
Transverse dunes have been surveyed in satellite images

Fig. 6. Subscene of Landsat ETM+ in false colour (RGB, 4, 3, 2) showing an area of plateau with megadune; the arrow shows the prevailing wind direction.
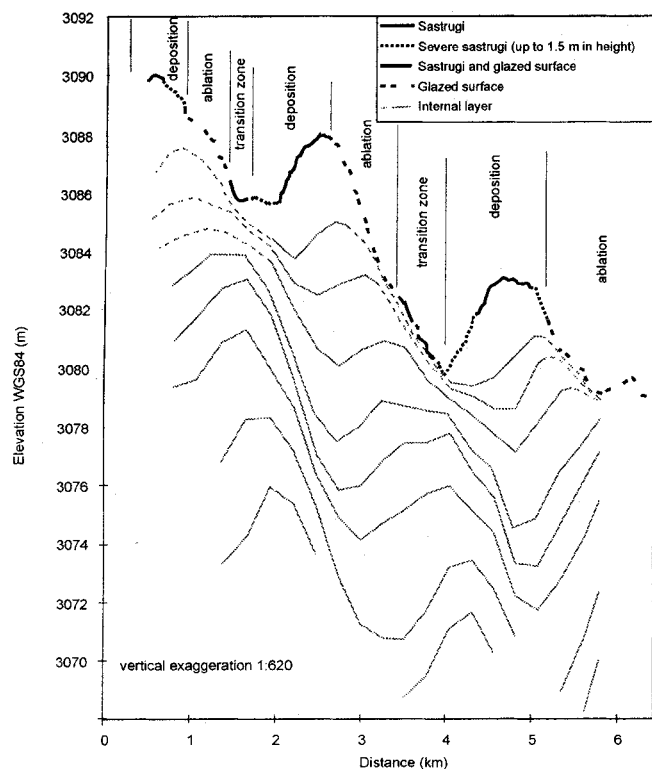
Fig. 7. Surface elevation, micro-relief morphology and internal layering along the megadune profile redrawn from Frezzotti and others (in press).

along the traverse between 2200 m a.s.l. (74°30' S, 153°20' E) and 3150 m a.s.l. (75°15' S, 127°20' E). Transverse dunes are present in sporadic areas between 2200 and 3000 m a.s.l.,

mainly downwind of the wide glazed surface (Fig. 2), where the surface decreases in slope and the atmosphere above the surface has a wave motion. Transverse dunes are perpendicular to the slope and similar to that reported by Black and Budd (1964) in Wilkes Land. Extensive presence of transverse dunes (>100 000 km^2), defined as megadunes, occurs along the traverse route between 75°27' S, 129°56' E and 75°25' S, 129°14' E (Fig. 6) and has been recognized by Fahnestock and others (2000b) and described in Frezzotti and others (in press). Megadune crests are found to be perpendicular to the prevailing katabatic wind direction but present an angle in the direction of the general surface slope at regional scale turning to the left under the action of the Southern Hemisphere Coriolis force (Frezzotti and others, in press).

The megadune surveyed along the traverse has a wavelength of about 3 km and an amplitude of 2–4 m, in agreement with the results of Fahnestock and others' (2000b) remote-sensing analysis. Glazed surfaces are located on the leeward slope of the megadune, while severe sastrugi (up to 1.5 m high) are located on the uphill slope (windward). Alternating sastrugi (up to 40 cm) and glazed surfaces are located at the bottom of the inter-dune area (Fig. 7). A buried megadune sedimentary structure (Fig. 7) has been surveyed by GPR–GPS (Frezzotti and others, in press). The presence of long-term hiatus surfaces (glazed surfaces) on the downwind faces of megadunes, and of accumulation–redistribution forms (severe sastrugi) on the uphill faces, suggests the surface migration of megadunes uphill (to windward). The uphill migration could be related to increased extension and uphill migration of severe sastrugi burying the slip face (long-term hiatus surfaces) of previous windward megadunes. Migration and ice-sheet
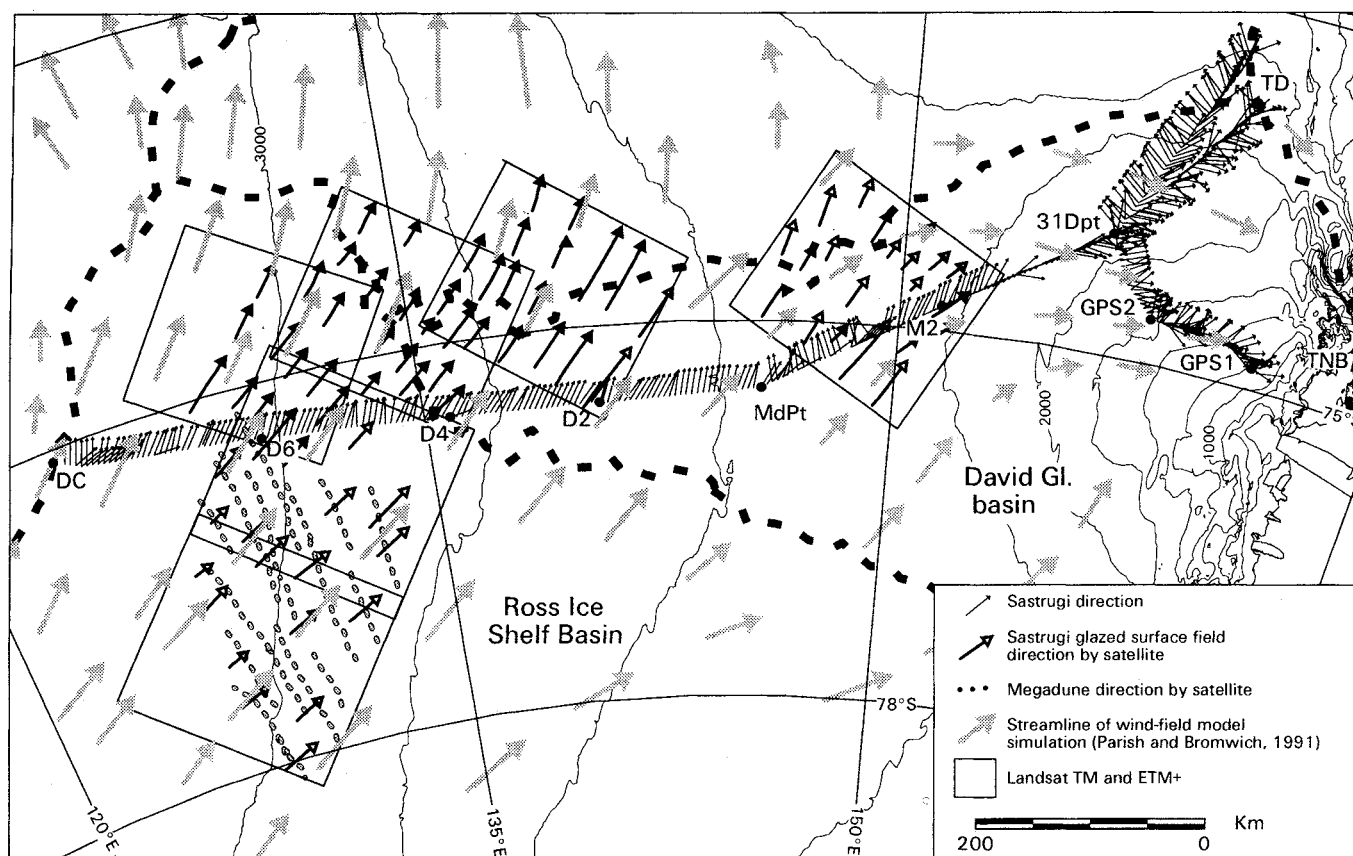

Fig. 8. Directions of sastrugi surveyed during the traverses; wind direction inferred from satellite images, satellite image location, streamlines of wind-field model simulation (Parish and Bromwich, 1991) and drainage basins.

surface flow (Bamber and others, 2000) show a close module (with the difference being due to the Coriolis force) but moving in the opposite direction and therefore having little or no absolute movement (Frezzotti and others, in press). This result supports the satellite observation by Fahnestock and others (2000b) that shows an identical pattern of branching and megadune expansion in images acquired 34 years apart with a maximum possible shift of $60 \, m \, a^{-1}$. Analysis of surface slope and satellite images indicated that the slope along prevalent wind direction and glazed surfaces is a crucial factor in the genesis of megadunes. Megadune formation could be explained by feedback between the megadune surface and the atmosphere. To explain the cyclic variation of the redistribution and erosion process of snow along a slope by an atmospheric wave, the atmospheric wavelength must be the same order of magnitude as the megadune (3–4 km). A gravity–inertia wave disturbing the geostrophic equilibrium of katabatic wind must be formed with weak amplitude (3–4 m), and the triggering occurs at the break in slope along the prevalent wind direction (Frezzotti and others, in press). Pettré and others (1986) hypothesized the formation of a gravity–inertia wave of 40 km, disturbing the geostrophic equilibrium, to explain periodic oscillations in accumulation at the break in slope 200 km from the Adélie Coast. Classification of the glazed surface and snow using Landsat ETM+ images indicated that the glazed surface covers about 20% of the megadune area.

These feedback systems between the cryosphere and atmosphere have important implications for the choice of sites for ice coring, because orographic variations of even a few metres per kilometre have a significant impact on the snow-accumulation process. The extensive presence of glazed surface caused by a long-term hiatus in accumulation, with a zero or slightly negative accumulation rate, has a significant impact on the surface mass balance of a wide area of the interior of East Antarctica.

Aeolian direction

The micro-relief directions measured on the field are parallel to the directions detected from the macro- morphology survey inferred from satellite images (Fig. 8). However, the field-inferred directions show the surface wind pattern in much greater detail and reveal areas of diffluence, divergence and confluence as a result of mesoscale topography. Satellite image data provide a large spatial coverage and are more representative at the regional scale. Directions detected in the field and by satellite data generally follow the predicted katabatic wind-field surface (Parish and Bromwich, 1991) from MdPt to DC (higher plateau); more differences are present in the confluence zone from MdPt to GPS1 over relatively steep slopes and mainly between M2 and 31Dpt. The difference between the observational and model (Parish and Bromwich, 1991) results could be related to the coarse spatial resolution of the model (50 km) and the inaccuracies of the surface topography (Drewry, 1983) used for modelling (Bamber and Huybrechts, 1996). Sastrugi and macro-morphology surveys show an angle between the wind direction and the direction of general surface slope at regional scale (Fig. 8). The difference between wind direction and slope decreases from the interior of the plateau (DC) to the confluence area of TNB. Wind direction turns to the left under the action of the Coriolis force in the high plateau, and becomes

directed in a more downslope direction near the steep coastal ice slopes in response to the sudden enhancement in the katabatic acceleration (Bromwich and others, 1990). The surface relief in the region from GPS1 to MdPt is oriented in two main directions. Micro-relief of a redistribution type is oriented parallel to the maximum slope, while micro- relief of the depositional type is oriented 30–70° off maximum slope. It is highly probable that the surface relief of the depositional type is formed by cyclonic storms, while that of the redistribution type is formed by katabatic winds. Near the dome area (TD and DC) the snow surface becomes smooth, with micro-reliefs oriented in two main directions.

ACKNOWLEDGEMENTS

REFERENCES

Bamber, J. L. and P. Huybrechts. 1996. Geometric boundary conditions for modelling the velocity field of the Antarctic ice sheet. *Ann. Glaciol.*, **23**, 364–373.

Bamber, J. L., D. G. Vaughan and I. Joughin. 2000. Widespread complex flow in the interior of the Antarctic ice sheet. *Science*, **287**(5456), 1248–1250.

Black, H. P. and W. Budd. 1964. Accumulation in the region of Wilkes, Wilkes Land, Antarctica. *J. Glaciol.*, **5**(37), 3–15.

British Antarctic Survey (BAS), Scott Polar Research Institute (SPRI) and World Conservation Monitoring Centre (WCMC). 1993. *Antarctic digital database user's guide and reference manual.* Cambridge, Scientific Committee on Antarctic Research.

Bromwich, D. H., T. R. Parish and C. A. Zorman. 1990. The confluence zone of the intense katabatic winds at Terra Nova Bay, Antarctica, as derived from airborne sastrugi surveys and mesoscale numerical modeling. *J. Geophys. Res.*, **95**(D5), 5495–5509.

Drewry, D. J. 1983. *Antarctica: glaciological and geophysical folio.* Cambridge, University of Cambridge. Scott Polar Research Institute.

Fahnestock, M. A., T. A. Scambos, R. A. Bindschadler and G. Kvaran. 2000a. A millennium of variable ice flow recorded by the Ross Ice Shelf, Antarctica. *J. Glaciol.*, **46**(155), 652–664.

Fahnestock, M. A., T. A. Scambos, C. A. Shuman, R. J. Arthern, D. P. Winebrenner and R. Kwok. 2000b. Snow megadune fields on the East Antarctic Plateau: extreme atmosphere–ice interaction. *Geophys. Res. Lett.*, **27**(22), 3719–3722.

Frezzotti, M. 1998. Surface wind field of Victoria Land (Antarctica) from surveys of aeolian morphologic features. *Terra Antartica Reports* 1, 1997, 43–45.

Frezzotti, M., O. Flora and S. Urbini. 1998. The Italian ITASE expedition from Terra Nova station to Talos Dome. *Terra Antartica Reports* 2, 105–108.

Frezzotti, M., I. E. Tabacco and A. Zirizzotti. 2000. Ice discharge of eastern Dome C drainage area, Antarctica, determined from airborne radar survey and satellite image analysis. *J. Glaciol.*, **46**(153), 253–264.

Frezzotti, M., S. Gandolfi and S. Urbini. In press. Snow megadune in Antarctica: sedimentary structure and genesis. *J. Geophys. Res.*

Fujii, Y. and K. Kusunoki. 1982. The role of sublimation and condensation in the formation of ice sheet surface at Mizuho Station, Antarctica. *J. Geophys. Res.*, **87**(C6), 4293–4300.

Fujiwara, K. and Y. Endo. 1971. Preliminary report of glaciological studies.

In Murayama, M., *ed. Report of the Japanese traverse, Syowa–South Pole 1968–69.* Tokyo, National Science Museum. Polar Research Centre, 71–104.

Goodwin, I. D. 1990. Snow accumulation and surface topography in the katabatic zone of eastern Wilkes Land, Antarctica. *Antarct. Sci.*, 2(3), 235–242.

Gow, A. J. 1965. On the accumulation and seasonal stratification of snow at the South Pole. *J. Glaciol.*, 5(40), 467–477.

Houbolt, J. J. 1968. Recent sediments in the southern bight of the North Sea. *Geol. Mijnbouw*, 47(4), 245–273.

Orheim, O. and B. K. Lucchitta. 1987. Snow and ice studies by Thematic Mapper and multispectral scanner Landsat images. *Ann. Glaciol.*, 9, 109–118.

Parish, T. R. and D. H. Bromwich. 1991. Continental-scale simulation of the Antarctic katabatic wind regime. *J. Climate*, 4(2), 135–146.

Pettré, P., J. F. Pinglot, M. Pourchet and L. Reynaud. 1986. Accumulation distribution in Terre Adélie, Antarctica: effect of meteorological parameters. *J. Glaciol.*, 32(112), 486–500.

Rémy, F., P. Shaeffer and B. Legrésy. 1999. Ice flow physical processes derived from ERS-1 high-resolution map of Antarctica and Greenland ice sheet. *Geophys. J. Int.*, 139(3), 645–656.

Richardson, C. and P. Holmlund. 1999. Spatial variability at shallow snow-layer depths in central Dronning Maud Land, East Antarctica. *Ann. Glaciol.*, 29, 10–16.

Richardson, C., E. Aarholt, S.-E. Hamran, P. Holmlund and E. Isaksson. 1997. Spatial distribution of snow in western Dronning Maud Land, East Antarctica, mapped by a ground-based snow radar. *J. Geophys. Res.*, 102(B9), 20,343–20,353.

Stenni, B. *and 6 others.* In press. Eight centuries of volcanic signal and climate change at Talos Dome (East Antarctica). *J. Geophys. Res.*

Urbini, S., S. Gandolfi and L. Vittuari. 2001. GPR and GPS data integration: examples of application in Antarctica. *Ann. Geofis.*, 44(4), 687–702.

Van den Broeke, M. R. and R. Bintanja. 1995. The interaction of katabatic winds and the formation of blue-ice areas in East Antarctica. *J. Glaciol.*, 41(138), 395–407.

Vaughan, D. G., H. F. J. Corr, C. S. M. Doake and E. D. Waddington. 1999. Distortion of isochronous layers in ice revealed by ground-penetrating radar. *Nature*, 398(6725), 323–326.

Warren, S. G. 1982. Optical properties of snow. *Rev. Geophys. Space Phys.*, 20(1), 67–89.

Watanabe, O. 1978. Distribution of surface features of snow cover in Mizuho Plateau. *Mem. Natl. Inst. Polar Res.*, Special Issue 7, 154–181.